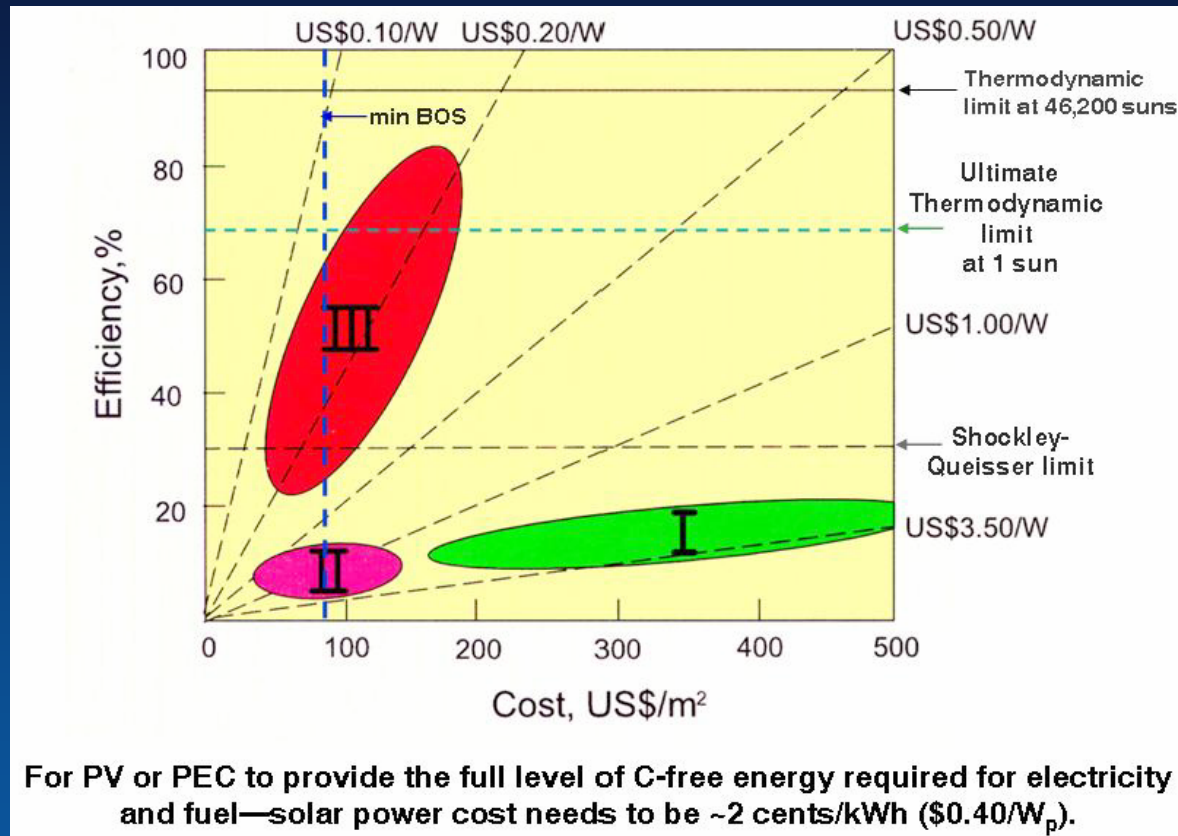


Intermediate Band Quantum Dot Solar Cells

**Mowafak Al-Jassim, Andrew Norman,
and Mark Hanna**

**National Center for Photovoltaics
National Renewable Energy Laboratory
Golden, Colorado**

PV power costs (\$/Wp) as a function of module efficiency and areal cost (Martin Green, 2004)



The biggest challenge is dramatically reducing the cost/watt of delivered solar electricity

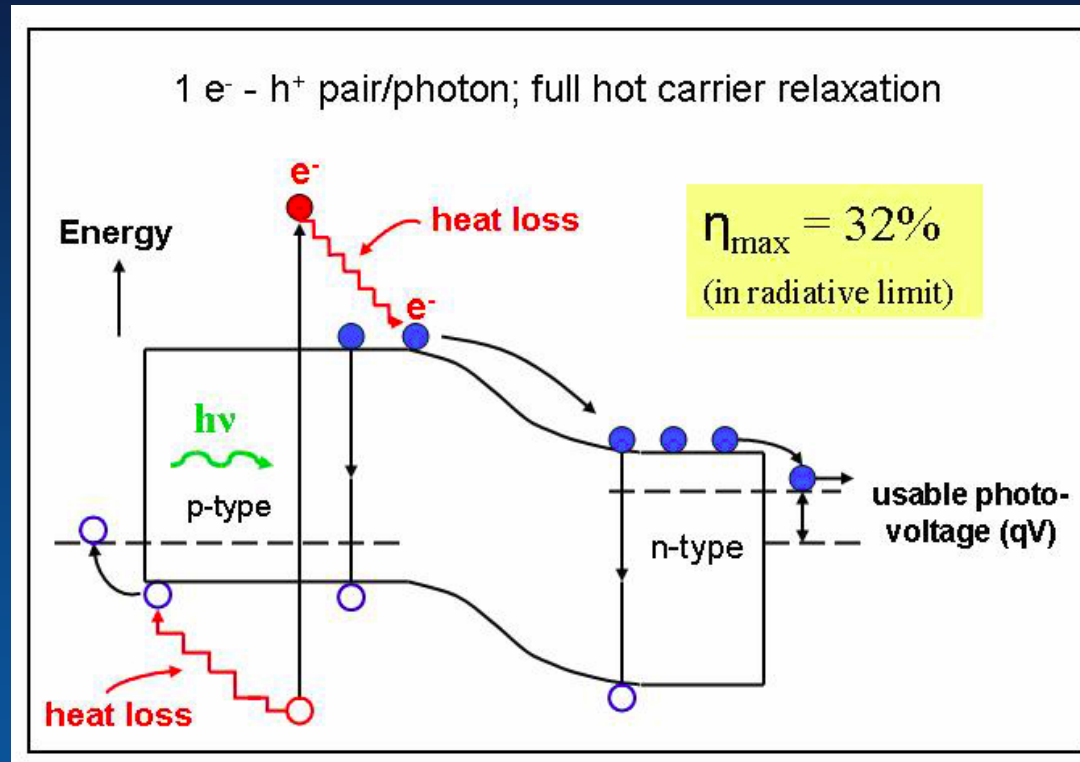
Third-generation PV

- Materials costs and availability are driving the evolution of PV technology towards a “third generation” of low-cost devices operating at efficiencies exceeding single-junction devices
- Possible approaches include:
 - Tandem cells: **the only proven technology so far**
 - Hot-carrier cells
 - Multiple-exciton-generation cells
 - Multiple-energy-level cells, **e.g., intermediate-band cells**
 - Thermophotovoltaic and thermophotonic conversion
- *See: Third Generation Photovoltaics: Advanced Solar Energy Conversion*, Prof. Martin A. Green, Springer-Verlag (Berlin, Heidelberg, 2003)

Next Generation Photovoltaics: High Efficiency through Full Spectrum Utilization, edited by A. Martí and A. Luque, Inst. of Physics (Bristol, 2004)

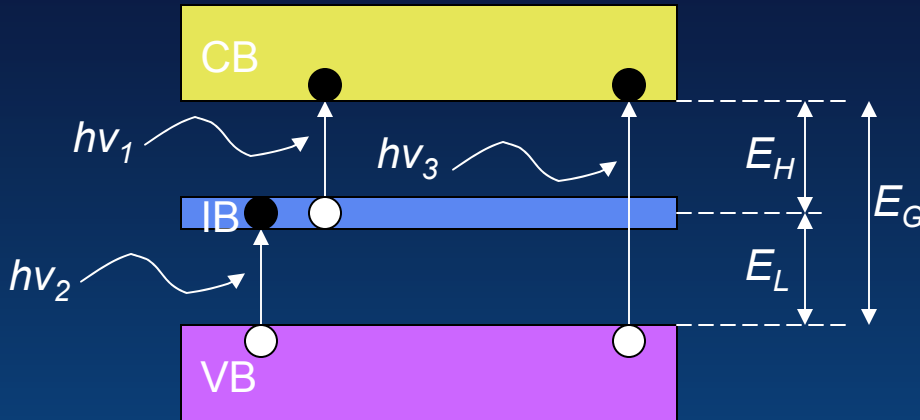
Limiting efficiency of single-junction solar cells

(Detailed balance calculations: Shockley and Queisser
J. Appl. Phys. 32 [1961] 510)



- Excess energy of photons absorbed with energies greater than semiconductor bandgap are lost as heat
- Photons with energies less than semiconductor bandgap are not absorbed

Intermediate-band solar cells (IBSC)



A. Luque and A. Martí, Phys. Rev. Lett. **78**, 5014 (1997)

Optimum gaps for maximum efficiency under maximum concentration conditions at 300 K:

$$E_L = 0.71 \text{ eV}$$

$$E_H = 1.24 \text{ eV}$$

$$E_G = 1.95 \text{ eV}$$

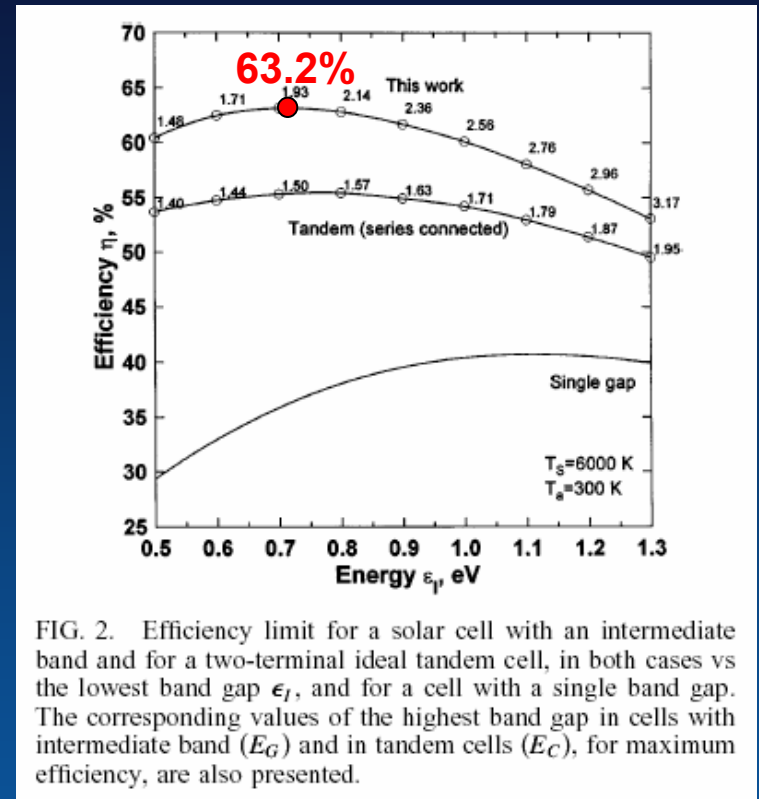


FIG. 2. Efficiency limit for a solar cell with an intermediate band and for a two-terminal ideal tandem cell, in both cases vs the lowest band gap ϵ_l , and for a cell with a single band gap. The corresponding values of the highest band gap in cells with intermediate band (E_G) and in tandem cells (E_C), for maximum efficiency, are also presented.

Maximum theoretical efficiency:

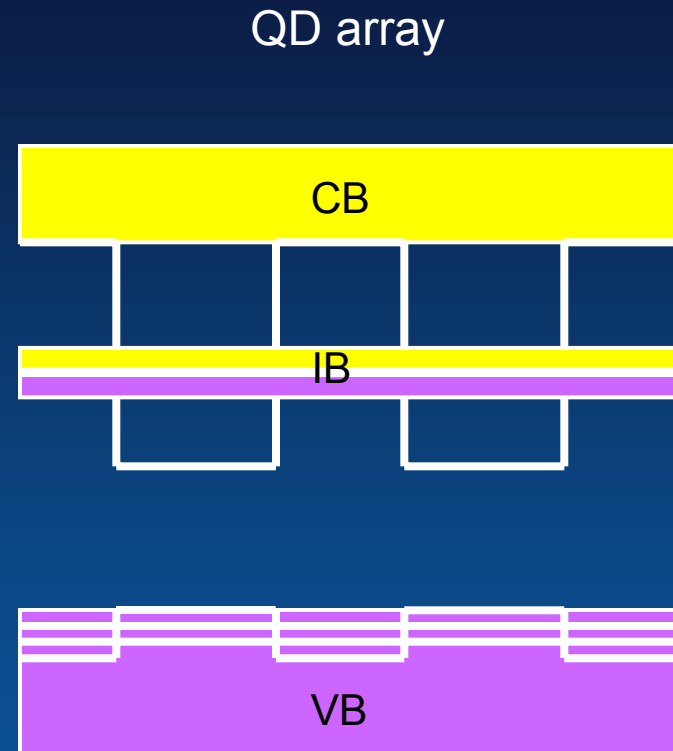
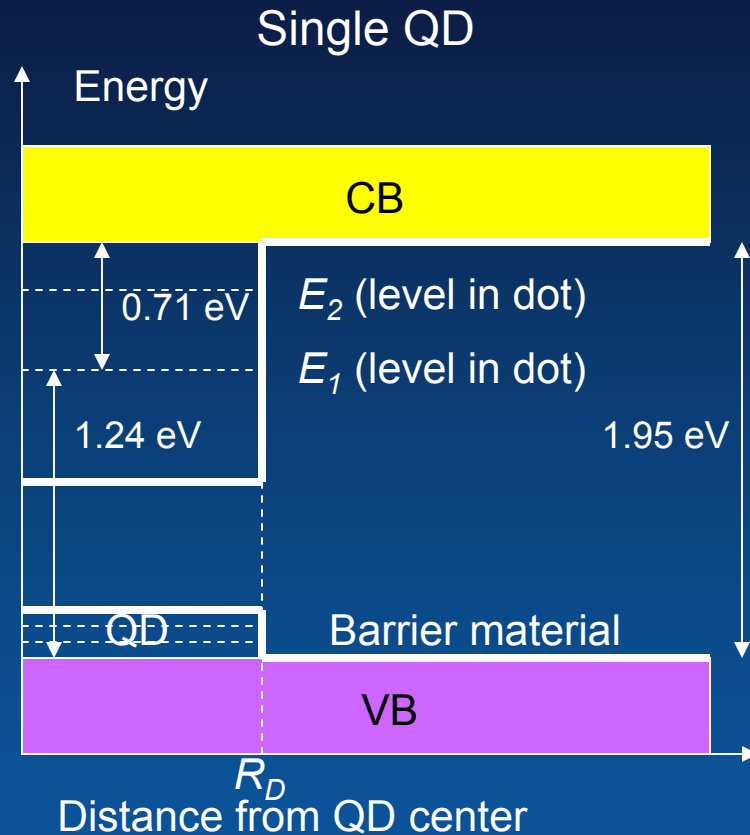
Single-gap solar cell = 40.7%

IBSC = 63.2%

Possible intermediate-band solar cell materials

- **Diluted II-VI oxide semiconductors**
e.g., $\text{Zn}_{1-y}\text{Mn}_y\text{O}_x\text{Te}_{1-x}$ alloys
Wu et al., Phys. Rev. Lett. **91** (2003) 246403
- **Transition-metal impurities in semiconductors**
e.g., $\text{Ga}_4\text{P}_3\text{M}$ and $\text{Ga}_x\text{P}_y\text{M}$ alloys, where M is a transition metal such as Ti
Wahnon and Tablero, Phys. Rev. B **65** (2002) 165115
Tablero, Phys. Rev. B **72** (2005) 035213
- **Quantum dots, e.g., InGaAs/(Al)GaAs**
Martí et al., Physica E **14** (2002) 150
Luque et al., J. Appl. Phys. **96** (2004) 903

Quantum dot intermediate-band solar cells (A. Martí et al., 2000)



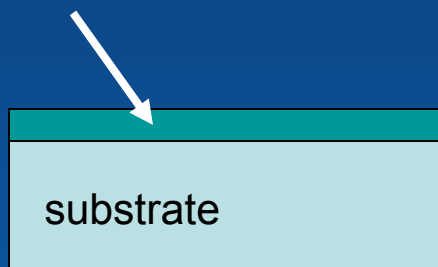
- Form an intermediate band by growing a close-packed ordered array of quantum dots
- Candidate materials: $\text{Al}_{0.4}\text{Ga}_{0.6}\text{As}$ barriers/ InGaAs QDs, but this system has large valence-band offset

Growth of quantum dot superlattices

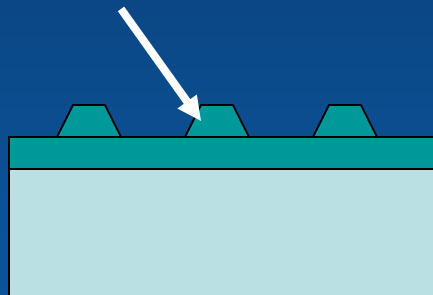
- Epitaxial growth by MBE or MOCVD using the strain-induced Stranski-Krastanov (SK) process, e.g., InGaAs/GaAs
- MOCVD is currently the preferred growth technique for high-efficiency multijunction solar cells

$$a_{\text{Layer}} > a_{\text{Substrate}}$$

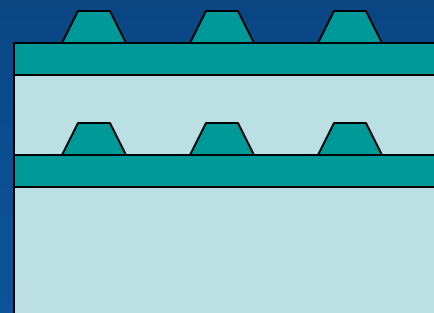
Initial growth of 2D strained wetting layer



After exceeding critical thickness, nucleation of 3D strained islands



If barrier layers are thin, strain coupling results in vertical stacking of subsequent QD layers

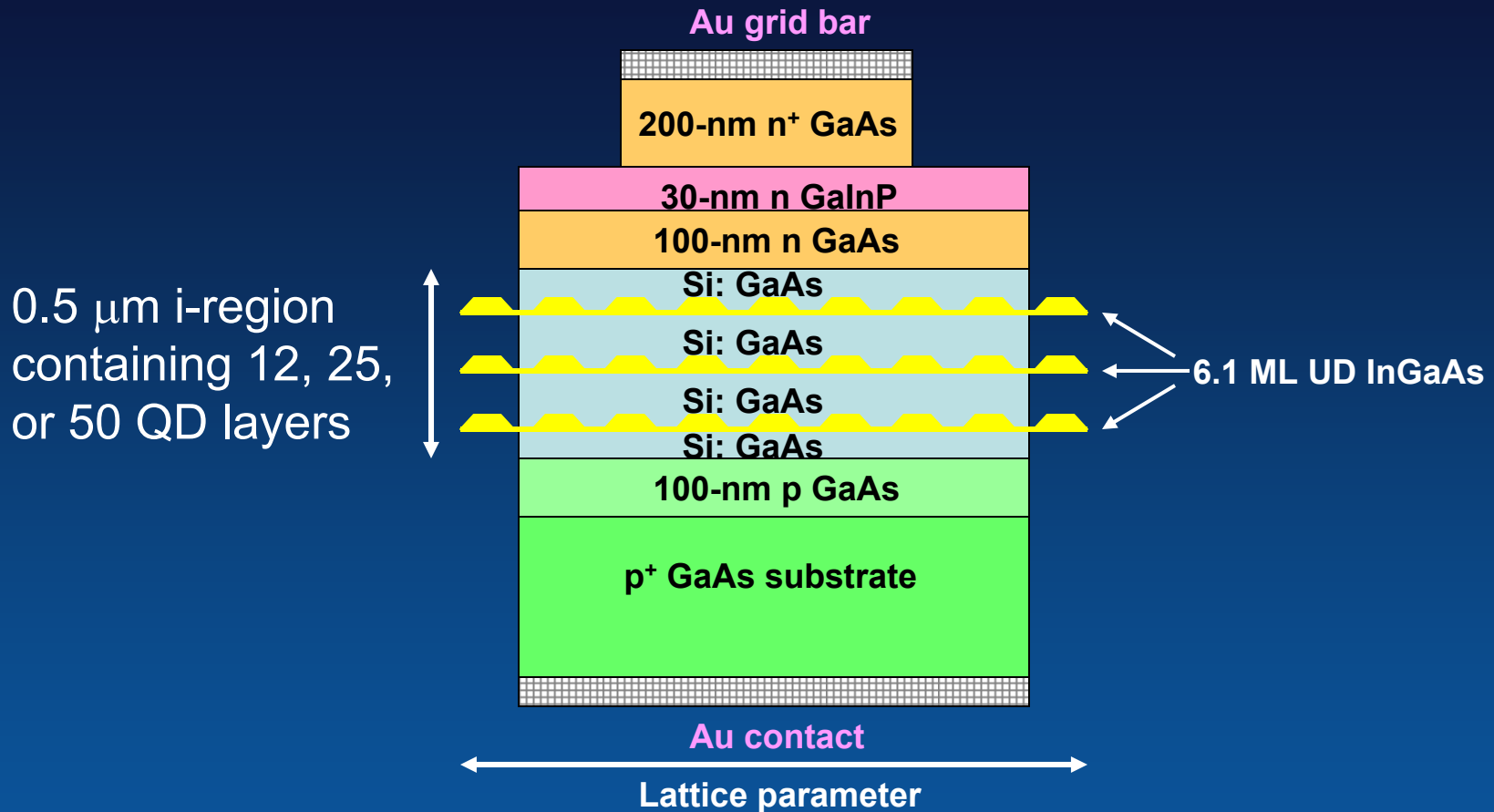


- 3D island formation is driven by a reduction in strain energy that outweighs the increase in surface energy that occurs

Some important characteristics of QDs for IBSC

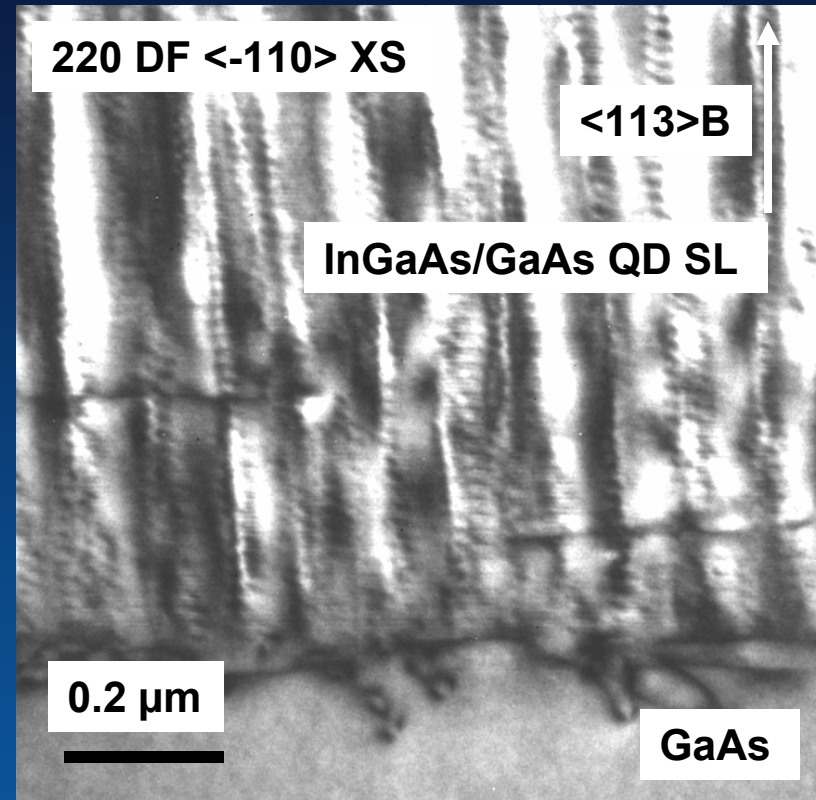
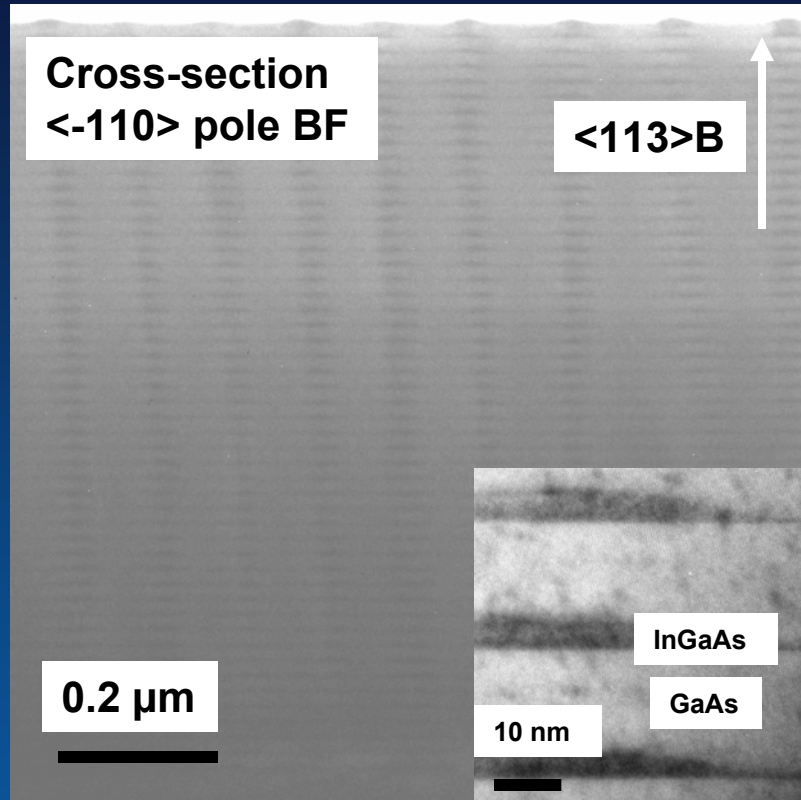
- **Dot size, shape, composition:** Suitable to obtain confined energy level in optimum position
- **Dot spacing:** Ideally require very close-packed 3D array of QDs
 - (a) So that wave functions of carriers in individual QDs overlap with each other and discrete energy levels of single QDs broaden into mini-bands
 - (b) To obtain a high absorption coefficient
- **Dot regularity:** Size dispersion $< 10\%$
- **Materials:** QDs and barrier layers with the optimum bandgap values, and good transport properties
- **Doping:** The IB needs to be partially-filled with electrons

InGaAs/GaAs QD superlattice (SL) *pin* solar cell



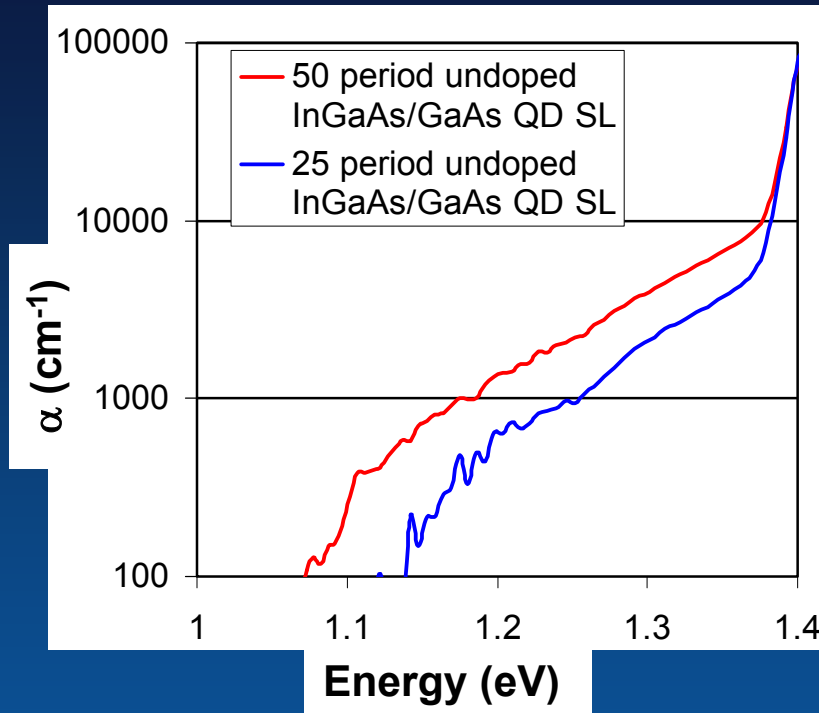
- Require QD SL with a high number of periods to maximize absorption and low defect density to minimize non-radiative recombination
- For InGaAs/GaAs QD SL with a large number of periods, the lattice mismatch with the substrate results in the generation of a high density of misfit dislocations that degrades cell performance

TEM of 50-period undoped MOCVD $\text{In}_{0.47}\text{Ga}_{0.53}\text{As}$ (6.1 ML)/GaAs (20 nm) QD SL on $\{113\}\text{B}$ GaAs



- Vertically stacked quantum dots through whole superlattice thickness along close to $\langle 113 \rangle \text{B}$
- High density of harmful dislocations present due to lattice mismatch between QD superlattice and GaAs substrate

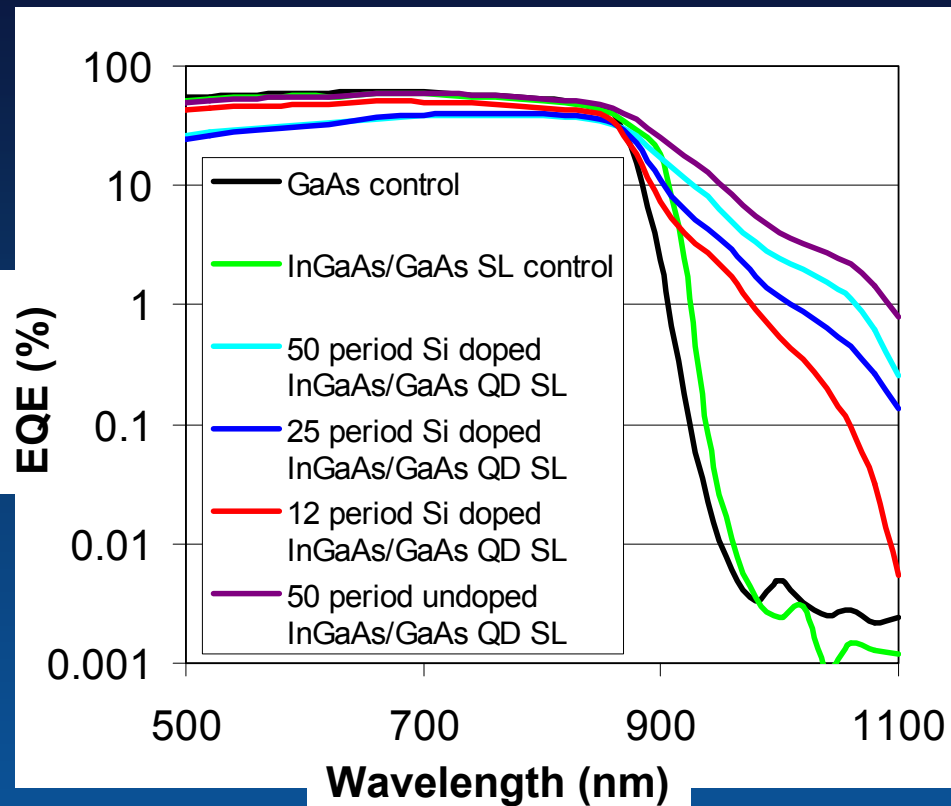
Absorption measurements on undoped $\text{In}_{0.47}\text{Ga}_{0.53}\text{As}/\text{GaAs}$ QD SLs



Absorption of sub-bandgap photons associated with VB-to-IB transition in QDs

- Weak absorption from InGaAs QDs starting at energy of ~ 1.1 eV
- Strength of absorption increases with increasing number of periods in QD SL

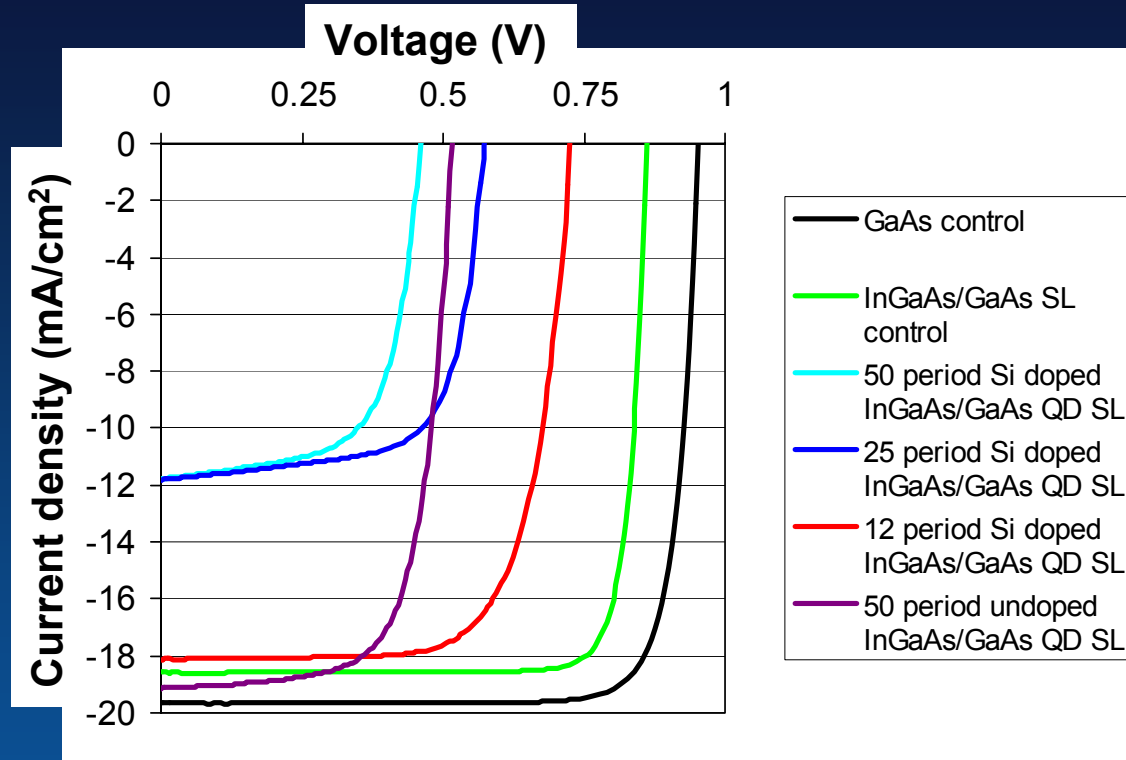
External quantum efficiencies (EQE) measured for cells grown on {113}B GaAs



Current generated by absorption of sub-bandgap photons associated with VB-to-IB transition in QDs

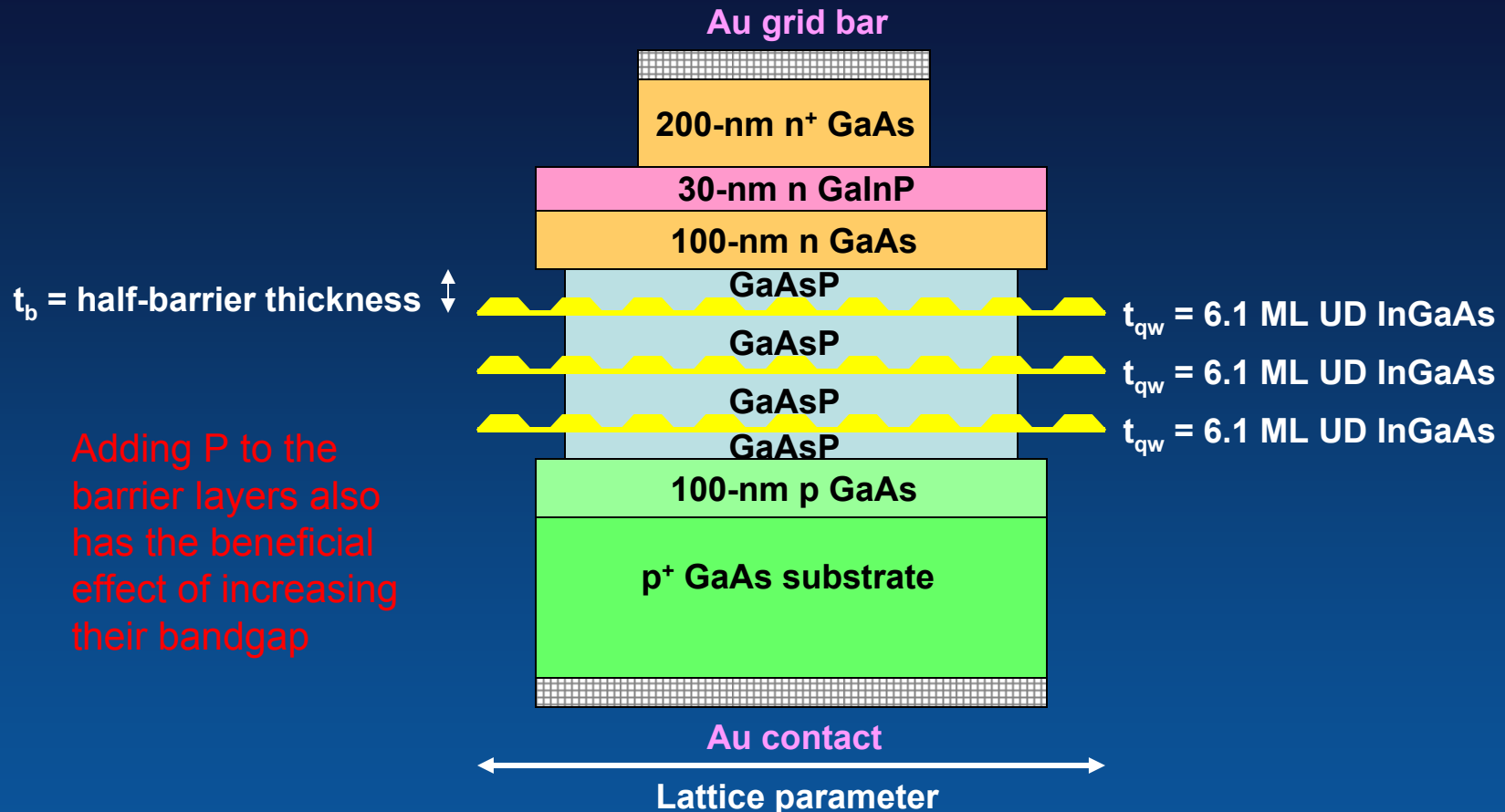
- QD SL devices have photoresponses extended to longer wavelengths than control cells due to absorption of sub-bandgap photons in QDs
- As the number of QD SL periods increases, the EQE increases for Si-doped structures at long wavelengths

Light IV curves measured under one-sun illumination for cells grown on {113}B GaAs



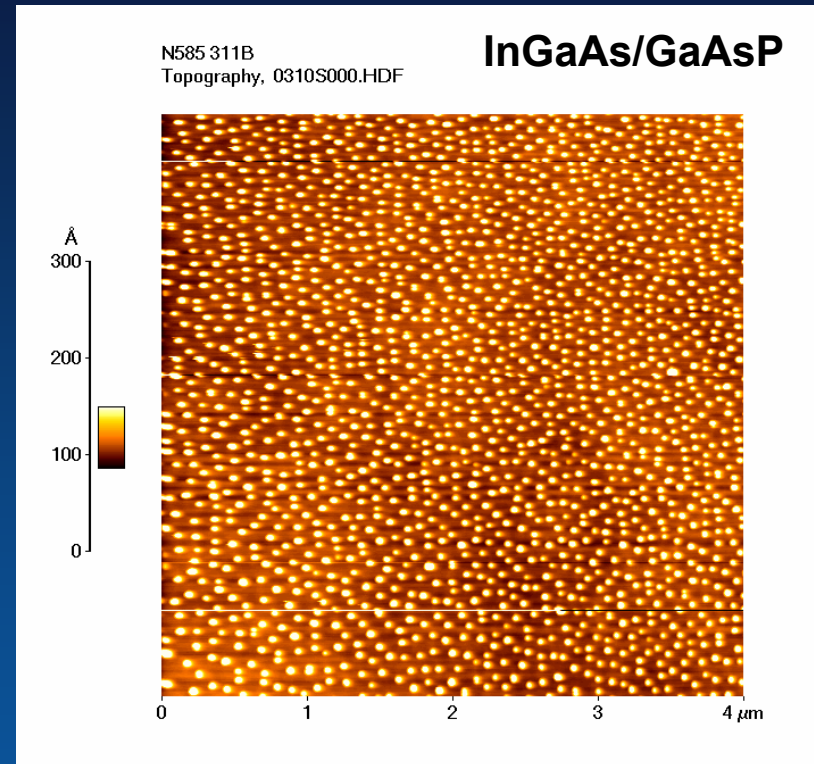
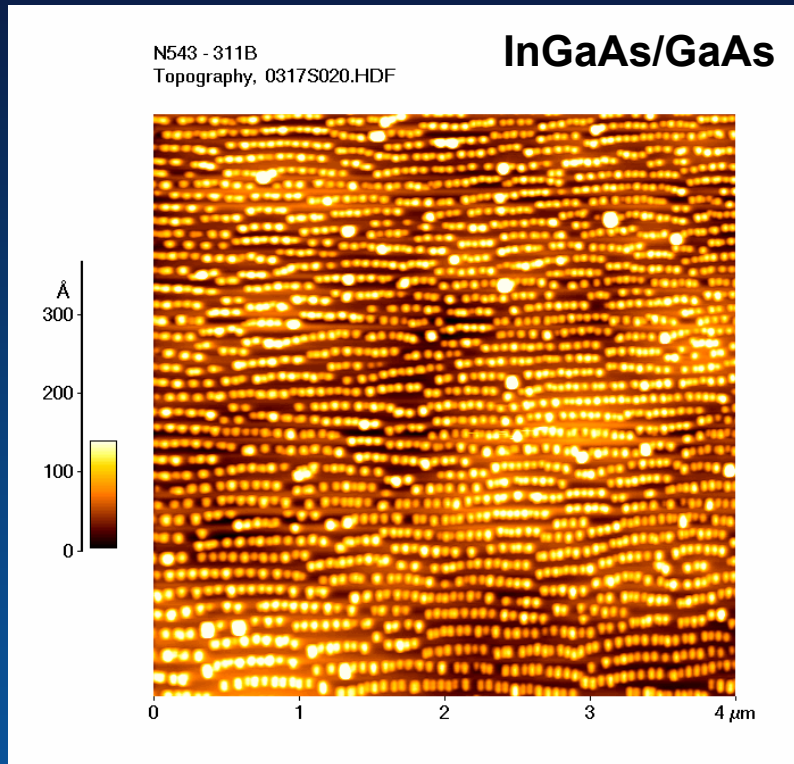
- InGaAs/GaAs SL and QD SL cells show reduced V_{oc} in comparison to GaAs control cell
- V_{oc} decreases as number of periods is increased for Si doped QD SL cells
- 25- and 50-period doped QD SL cells also have much reduced J_{sc} values in comparison to control cells and 12-period doped QD SL cell
- 50-period undoped QD SL cell has J_{sc} comparable to control cells

Strain-balanced QD SLs to avoid misfit dislocations



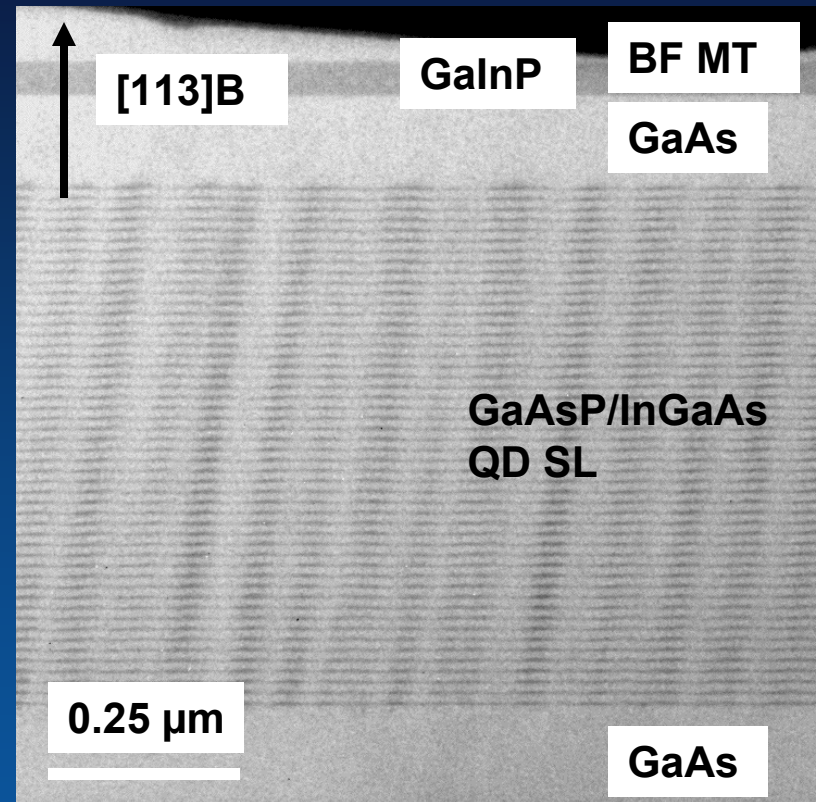
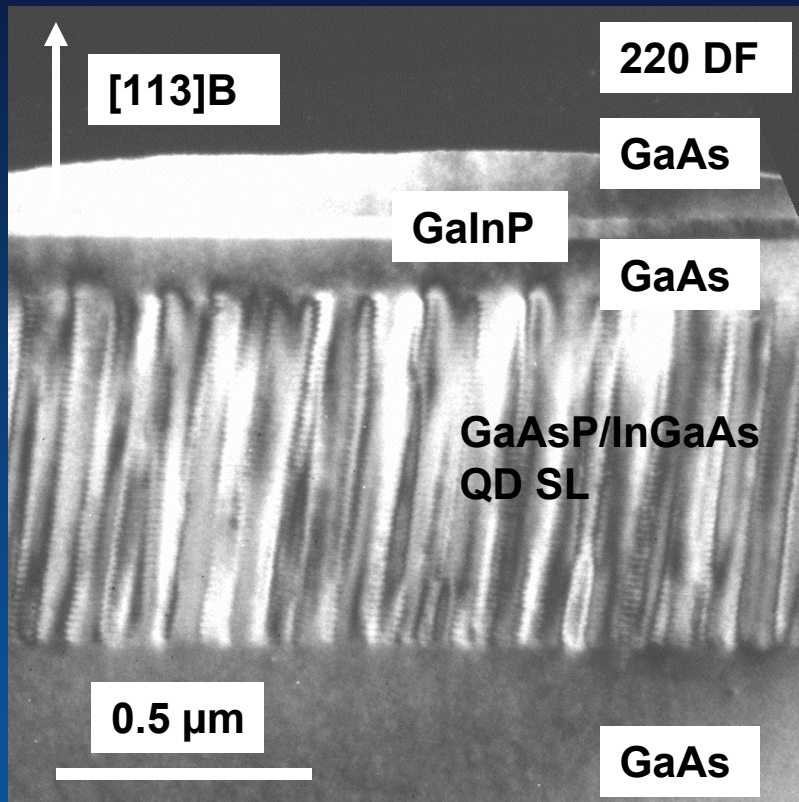
- Compressive strain of InGaAs QD layers is compensated by tensile GaAsP layers such that average lattice parameter of QD SL is equal to GaAs substrate
- $\langle a \rangle = \frac{2t_b a_{\text{GaAsP}} + t_{qw} a_{\text{InGaAs}}}{2t_b + t_{qw}}$ (Ekins-Daukes et al., APL **75** [1999], 4195)

AFM of 50-period InGaAs (6.1 ML)/GaAs (20 nm) and 20-period InGaAs (6.1 ML)/GaAsP (20 nm, 8.3% P) QD SL incorporating 30-second H₂ anneal after each QD layer



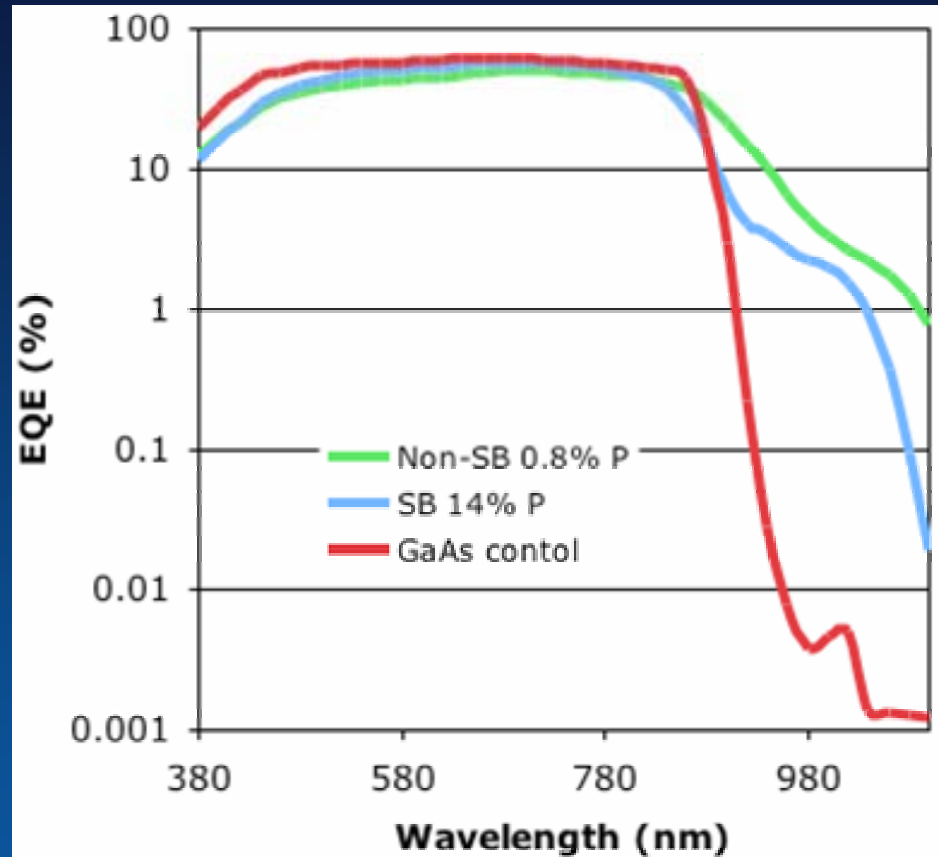
- **InGaAs/GaAs**: Rows of ordered QDs present aligned along $[-110]$, QD density $\sim 10^{10} \text{ cm}^{-2}$
- **InGaAs/GaAsP**: No lateral ordering of QDs, QD density $\sim 10^{10} \text{ cm}^{-2}$

Cross-section TEM of 50-period, undoped SB InGaAs/GaAsP QD SL with 14% P in barrier layers



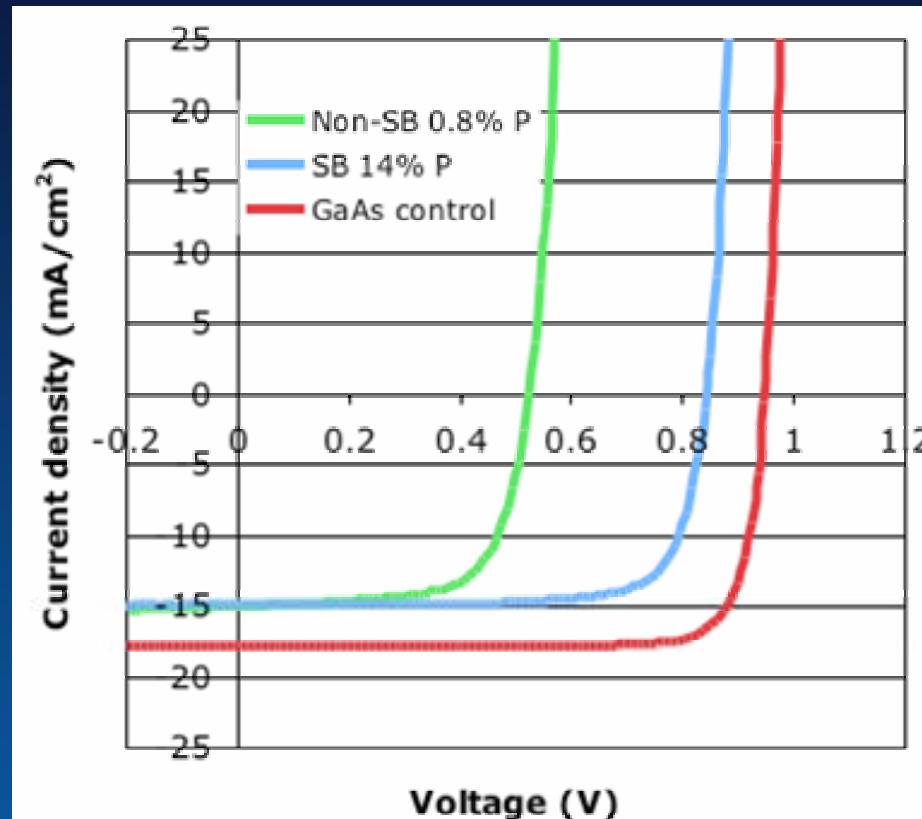
- No misfit or threading dislocations present
- See nearly vertical columns of InGaAs QDs through all 50 periods

External quantum efficiencies (EQE) measured for SB and non-SB InGaAs/GaAsP QD SL cells



- The InGaAs/GaAsP QD SL devices have photoresponses extended to longer wavelengths than GaAs control cells
- Increasing the amount of P in the barrier layers shifts the photoresponse cut-off to shorter wavelengths

Light IV curves: Higher V_{oc} obtained by growth of strain-balanced structures



- Adding P to barrier layers to achieve strain balance leads to a significant increase in V_{oc} (partly due to the increase in bandgap of the barrier layers and partly due to reduction in dislocation density)
- The SB InGaAs/GaAsP QD SL cell still shows reduced J_{sc} and V_{oc} in comparison to GaAs control cell

What limits performance of these QD IBSC?

- **Weak absorption of sub-bandgap photons:** IB-to-CB absorption transition may be weak because of insufficient number of QDs in structures
- **Low open-circuit voltage:** Rapid relaxation and capture of carriers into QDs
- **Low currents:** QDs may be acting as traps for carriers lowering efficiency of carrier collection (will probably need a built-in electric field in intrinsic region of a *pin* device to help separate charge carriers and improve their collection, need to slow down carrier capture and recombination in QDs)
- **Cost:** Epitaxially grown QD structures are very expensive to produce; if concept works, then we may want to move to colloidal QD-based cells to lower cost

Conclusions

- We have achieved MOCVD growth of up to 50-period strain-balanced InGaAs/GaAsP QD SLs with lower defect densities and better optical properties than InGaAs/GaAs QD SLs
- Strain-balanced InGaAs/GaAsP QD SL solar cells show a significant increase in V_{OC} in comparison to InGaAs/GaAs QD SL cells
- QD SL cells show photoresponses extended to longer wavelengths than GaAs control cells, demonstrating current generation from the absorption of sub-bandgap photons

Conclusions

- IBSC theoretically offers a way to significantly increase cell efficiency compared to that of a single-junction solar cell
- Although some of the key operating principles of IBSC have been demonstrated, cell efficiencies have so far not exceeded the Shockley-Queisser limit for a single-junction solar cell
- Much more work needs to be done before IBSC can make a major contribution to the PV market